Two distinct myosin II populations coordinate ovulatory contraction of the myoepithelial sheath in the *Caenorhabditis elegans* somatic gonad

Kanako Ono and Shoichiro Ono*
Department of Pathology and Department of Cell Biology, Emory University, Atlanta, GA 30322

ABSTRACT **The myoepithelial sheath in the somatic gonad of the nematode *Caenorhabditis elegans* has nonstriated contractile actomyosin networks that produce highly coordinated contractility for ovulation of mature oocytes. Two myosin heavy chains are expressed in the myoepithelial sheath, which are also expressed in the body-wall striated muscle. The troponin/tropomyosin system is also present and essential for ovulation. Therefore, although the myoepithelial sheath has smooth muscle–like contractile apparatuses, it has a striated muscle–like regulatory mechanism through troponin/tropomyosin. Here we report that the myoepithelial sheath has a distinct myosin population containing nonmuscle myosin II isoforms, which is regulated by phosphorylation and essential for ovulation. MLC-4, a nonmuscle myosin regulatory light chain, localizes to small punctate structures and does not colocalize with large, needle-like myosin filaments containing MYO-3, a striated-muscle myosin isoform. RNA interference of MLC-4, as well as of its upstream regulators, LET-502 (Rho-associated coiled-coil forming kinase) and MEL-11 (a myosin-binding subunit of myosin phosphatase), impairs ovulation. Expression of a phosphomimetic MLC-4 mutant mimicking a constitutively active state also impairs ovulation. A striated-muscle myosin (UNC-54) appears to provide partially compensatory contractility. Thus the results indicate that the two spatially distinct myosin II populations coordinately regulate ovulatory contraction of the myoepithelial sheath.**

Monitoring Editor
Jeffrey D. Hardin
University of Wisconsin

Received: Sep 11, 2015
Revised: Feb 5, 2016
Accepted: Feb 5, 2016

INTRODUCTION

Contractility generated by the interaction of actin and myosin not only drives muscle contraction but also plays important roles in fundamental biological processes, including cell migration, cytokinesis, and tissue morphogenesis (Munjal and Lecuit, 2014; Zaidel-Bar *et al.*, 2015). The actin–myosin interaction is highly regulated by complex mechanisms to ensure that contractility is produced at the appropriate location and timing (Zaidel-Bar *et al.*, 2015). A type 2 myosin molecule (myosin II) is composed of two each of myosin heavy chain, myosin essential light chain, and myosin regulatory light chain (MRLC). In mammals, multiple myosin heavy chain isoforms are present and exhibit different biochemical properties and isoform-specific cellular functions (Beach and Hammer, 2015). This complexity provides cells a large number of ways to control actomyosin contractility using different regulatory components and myosin isoforms. Therefore any particular cell type could use multiple mechanisms to control contractility, and how they are coordinated to regulate a biological process is not understood in many cases.

The somatic gonad of the nematode *Caenorhabditis elegans* has several contractile tissues that provide essential forces to transport oocytes and embryos (Hubbard and Greenstein, 2000; Yamamoto *et al.*, 2006). The proximal ovary near the uterus houses oocytes that are surrounded by the myoepithelial sheath (Supplemental Figure S1). When the most proximal oocyte becomes mature, the myoepithelial sheath initiates intense contraction and expels the oocyte into the spermatheca, where fertilization takes place (McCarter *et al.*, 1997). Ovulatory contraction of the myoepithelial sheath is tightly coupled with oocyte maturation and regulated by major sperm protein from sperm (Miller *et al.*, 2001), a signal through gap

This article was published online ahead of print in MBoC in Press (http://www.molbiolcell.org/cgi/doi/10.1091/mbc.E15-09-0648) on February 10, 2016.

*Address correspondence to: Shoichiro Ono (sono@emory.edu).

Abbreviations used: Emo, endomitotic oocytes in the ovary; GFP, green fluorescent protein; IP3, inositol 1,4,5-triphosphate; MRLC, myosin regulatory light chain; p-MRLC, phosphorylated MRLC; RNAi, RNA interference; ROCK, Rho-associated coiled-coil–forming kinase.

junctions between the myoepithelial sheath and oocytes (Whitten and Miller, 2006), and epidermal growth factor–like signaling (Yin *et al.*, 2004). Downstream of these cell-surface events, inositol 1,4,5-triphosphate (IP3) signaling is triggered to enhance myoepithelial sheath contraction, presumably by increasing Ca^{2+} release (Yin *et al.*, 2004; Xu *et al.*, 2005, 2007). However, how these signaling processes finally regulate actomyosin interaction is unknown.

The myoepithelial sheath has nonstriated actomyosin networks and expresses UNC-54 and MYO-3 myosin heavy chains, which are the same myosin isoforms present in the thick filaments of *C. elegans* striated muscle (Strome, 1986; Ardizzi and Epstein, 1987). The myoepithelial sheath also has the troponin/tropomyosin system as essential factors for ovulation (Myers *et al.*, 1996; Ono and Ono, 2004; Obinata *et al.*, 2010). Given that the troponin/tropomyosin complex is typically the major Ca^{2+}-dependent switch for actomyosin interaction in striated muscle (Ebashi, 1984), a relatively simple hypothesis was that an IP3-mediated Ca^{2+} release relieves the inhibitory function of troponin for actomyosin interaction to induce ovulatory contraction. A study showed that VAV-1, a guanine nucleotide exchange factor for Rho small GTPase, regulates ovulatory contraction of the myoepithelial sheath by modulating IP3-mediated Ca^{2+} release (Norman *et al.*, 2005). However, the Rho small GTPase is known to have a conserved signaling function to regulate myosin activity independent of Ca^{2+} (Piekny *et al.*, 2005), and this pathway has not been explored in *C. elegans* ovulation.

Here we found that MLC-4, a nonmuscle isoform of MRLC, is assembled into small myosin puncta in the myoepithelial sheath, which are spatially distinct from previously known large, needle-like myosin filaments containing UNC-54 and MYO-3 myosin heavy chains. MLC-4, along with Rho-dependent myosin regulators, is essential for successful ovulation. These two distinct myosin populations apparently provide partially compensatory contractility in the ovulatory phase. Thus our results suggest that the MLC-4-containing myosin II is a Rho GTPase–regulated generator of contractility and that the two myosin II populations coordinate to produce actomyosin contractility for successful ovulation.

RESULTS

Nonmuscle/smooth-muscle myosin II subunits MLC-4 and NMY-2 localize to puncta that are spatially distinct from needle-like "striated-muscle" myosin filaments

Expression of the MLC-4 nonmuscle MRLC in the myoepithelial sheath of the somatic gonad has been briefly documented previously (Shelton *et al.*, 1999), but subcellular localization of MLC-4 has not been reported in detail. We found that MLC-4 localized to puncta in the myoepithelial sheath. Transgenically expressed green fluorescent protein (GFP)–tagged MLC-4 localized in a punctate pattern (Figure 1A). This localization pattern of MLC-4 appeared very different from those of "striated-muscle" myosin heavy chains MYO-3 (Figure 1C) and UNC-54, which coassemble large, needle-like, thick filaments with paramyosin cores (Ardizzi and Epstein, 1987; Rose *et al.*, 1997; Ono *et al.*, 2007). Spatial comparison of GFP–MLC-4 and MYO-3 revealed that they did not colocalize in the myoepithelial sheath (Figure 1, A, C, and G), suggesting that nonmuscle myosin containing MLC-4 and striated-muscle myosin containing MYO-3 form spatially distinct myosin filaments. The microscopic images were further analyzed by measuring Pearson's coefficient (PC), which is close to 1 when two images overlap perfectly and <0 when two images are exclusive (Bolte and Cordelieres, 2006). MYO-3 and F-actin are known to colocalize, and PC for the two images was ~0.3 (Figure 1I). PC for MLC-4 and F-actin was similar to that for MYO-3 and F-actin (Figure 1I), whereas PC for MLC-4 and MYO-3 was ~0 and significantly lower than that for MYO-3 and F-actin (Figure 1I). Therefore MYO-3 and MLC-4 do not colocalize, but they are associated with F-actin, perhaps in different regions of the actin networks.

Furthermore, we found that the GFP-tagged NMY-2 nonmuscle myosin heavy chain also localized in a punctate pattern in the myoepithelial sheath in a similar manner to MLC-4 (Figure 1B). Similarly, the NMY-2 puncta did not colocalize with MYO-3 myosin heavy chain (Figure 1, B, D, and H). Because MLC-4 is the sole nonmuscle MRLC in *C. elegans* (Shelton *et al.*, 1999), the similar localization patterns of MLC-4 and NMY-2 strongly suggest that they coassemble small myosin II filaments in the myoepithelial sheath. However, because both MLC-4 and NMY-2 were tagged with GFP, their colocalization was not examined. Quantitative analysis showed that PC for NMY-2 and F-actin was similar to that for MYO-3 and F-actin, whereas PC for NMY-2 and MYO-3 was ~0 and significantly lower than that for MYO-3 and F-actin (Figure 1I). The results indicate that NMY-2 colocalized with F-actin but not with MYO-3. These observations indicate that nonmuscle/smooth-muscle myosin and striated-muscle myosin form spatially distinct populations of myosin II filaments in the myoepithelial sheath.

To determine whether striated-muscle myosin and nonmuscle myosin are associated with a common actin network or separate pools of actin bundles, we traced 6–9 μm of MYO-3–associated actin bundles and counted the numbers of spots of GFP–MLC-4 and GFP–NMY-2. We found that each MYO-3–associated actin bundle was also associated with spots of GFP–MLC-4 and GFP–NMY-2 with average intervals of 2.4 ± 0.48 (n = 10) and 2.3 ± 0.29 μm (n = 10), respectively. Representative actin bundles associated with both MYO-3 and GFP-MLC-4 or GFP-NMY-2 are shown in insets in Figure 1, G and H. These results suggest that striated-muscle myosin and nonmuscle myosin are associated with a common actin network in different regions.

The MLC-4 myosin regulatory light chain is required for ovulation

Previous studies showed that striated-muscle myosin heavy chains MYO-3 and UNC-54 play important roles in ovulatory contraction of the myoepithelial sheath (Rose *et al.*, 1997; Ono *et al.*, 2007). However, roles of the MLC-4 nonmuscle MRLC in the myoepithelial sheath have not been examined. To determine whether MLC-4 is involved in ovulation, we examined effects of MLC-4 knockdown by RNA interference (RNAi). *mlc-4(RNAi)* in wild-type background caused severe morphological defects in the entire gonads, including the germline (unpublished data), which is consistent with the previously reported roles of MLC-4 and nonmuscle myosin heavy chains in embryonic cytokinesis and germline development (Shelton *et al.*, 1999; Piekny *et al.*, 2003; Kachur *et al.*, 2008). These strong phenotypes precluded us from examining *mlc-4(RNAi)* phenotypes specifically in the somatic gonad. Therefore we used the *ppw-1* mutant strain, which is defective in RNAi specifically in the germline lineage (Tijsterman *et al.*, 2002) and allowed us to examine soma-specific RNAi phenotypes.

RNA interference of *mlc-4* in *ppw-1* mutant caused accumulation of endomitotic oocytes in the proximal ovary (Emo phenotype) in 100 ± 0.0% (n = 3; 100 worms were scored in each experiment; Figure 2B, arrow), which is typically a result of repeated DNA replication cycles due to defective ovulation (Iwasaki *et al.*, 1996). Control RNAi in *ppw-1* did not cause significant abnormalities in the gonad (Emo phenotype, 0.67 ± 0.56%; n = 3; 100 worms scored in each experiment; Figure 2A), indicating that the *ppw-1* mutation did not affect the ovulation process. Of interest, the overall architecture

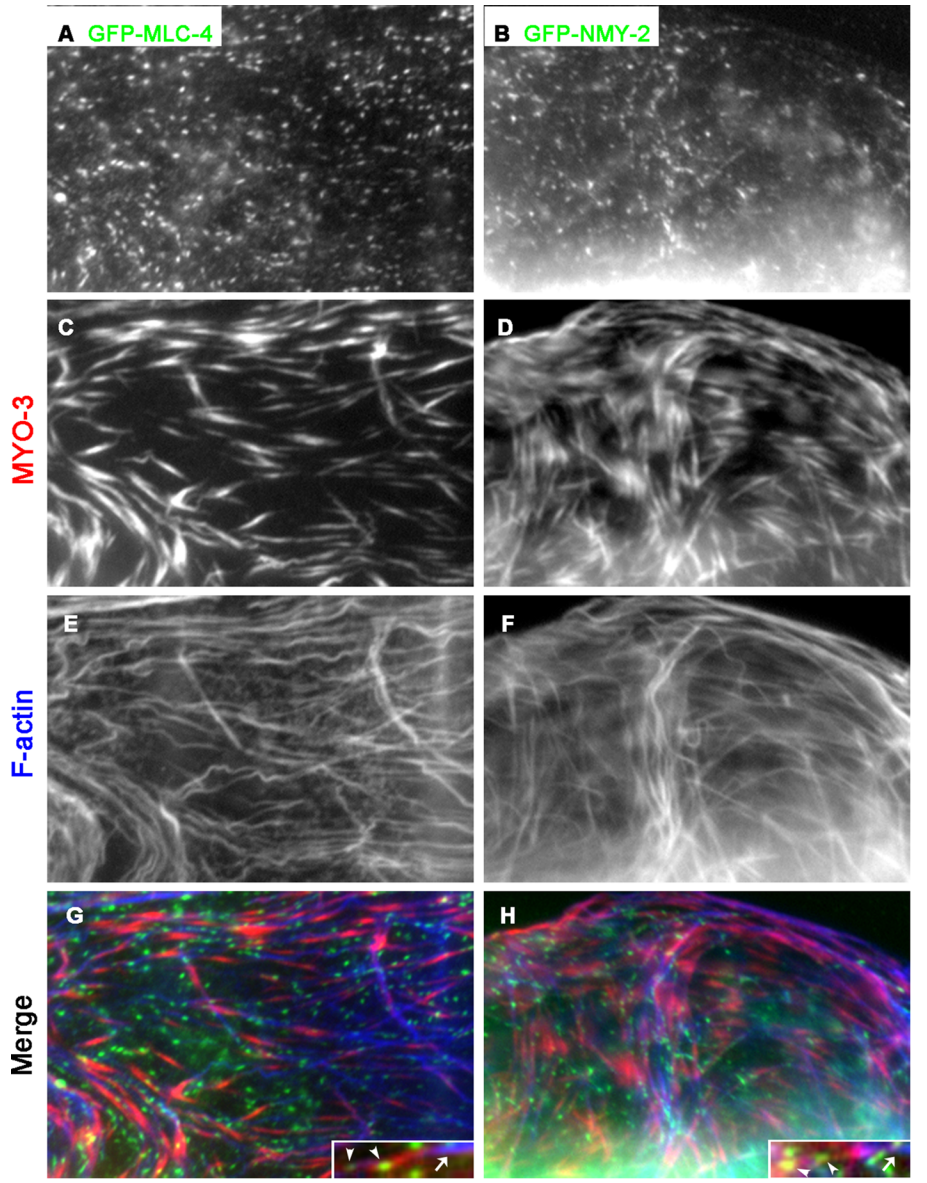

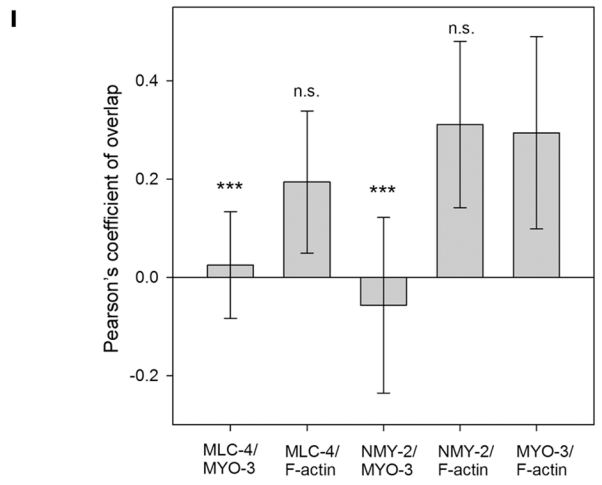

FIGURE 1: Nonmuscle myosin II isoforms localize to puncta and do not colocalize with large, needle-like muscle myosin filaments in the myoepithelial sheath. Dissected gonads from worms expressing GFP–MLC-4 (EU573; left) or GFP-NMY-2 (JJ1473; right) were stained for GFP (A, B), MYO-3 (C, D), and F-actin (E, F). Regions of the myoepithelial sheath. (G, H) Merged images (GFP in green, MYO-3 in red, and F-actin in blue). Insets, magnified images of representative actin bundles associated with both MYO-3 (arrows) and GFP–MLC-4 or GFP–NMY-2 (arrowheads). (I) Pearson's coefficient quantified as a measurement of colocalization for each pair of proteins, shown as average ± SD ($n = 11$). Results of a statistical test by one-way ANOVA for comparisons with MYO-3/F-actin as a control; n. s., not significant ($p > 0.05$); ***$p < 0.001$. The quantitative image analysis indicates that both GFP–MLC-4 and GFP–NMY-2 are associated with F-actin but not with MYO-3, suggesting spatial segregation of striated-muscle myosin and nonmuscle myosin.

of the networks of actin filaments and MYO-3 in the myoepithelial sheath was largely intact after depletion of MLC-4 (compare Figure 2, E and F), suggesting that MLC-4 is involved in contractility but not assembly of the actomyosin network.

Phosphoregulation of MLC-4 is required for ovulation

Regulation of myosin activity by phosphorylation and dephosphorylation of MRLC has been characterized in nonmuscle and smooth-muscle cells of metazoan species (Matsumura *et al.*, 2011). In *C. elegans*, *let-502* (Rho-associated coiled-coil–forming kinase [ROCK]) and *mel-11* (myosin-binding subunit of MRLC phosphatase) were identified as antagonistic regulators of cell or tissue contractility through MRLC (Wissmann *et al.*, 1997, 1999; Piekny *et al.*, 2000; Piekny and Mains, 2002; Gally *et al.*, 2009). Previous work demonstrated that *let-502* and *mel-11* have opposite roles in contractility of the spermatheca affecting fertility (Wissmann *et al.*, 1999). Therefore we examined whether these two genes are involved in contractility of the myoepithelial sheath, using the *ppw-1* mutant.

RNA interference of either *let-502* or *mel-11* in *ppw-1* mutant caused accumulation of endomitotic oocytes in the proximal ovary (Figure 2, C and D), suggesting strongly that these two myosin regulators are important for regulation of myoepithelial sheath contractility during ovulation. *let-502(RNAi)* in *ppw-1* caused the Emo phenotype (Figure 2C, arrow) in 31 ± 3.6% ($n = 3$). *mel-11(RNAi)* in *ppw-1* caused the Emo phenotype (Figure 2D, arrow) in 85 ± 3.0% ($n = 3$). The relatively low penetrance of the *let-502(RNAi)* phenotype suggests that there is an alternative mechanism to either phosphorylate/activate MLC-4 or provide actomyosin contractility. Alternatively, the

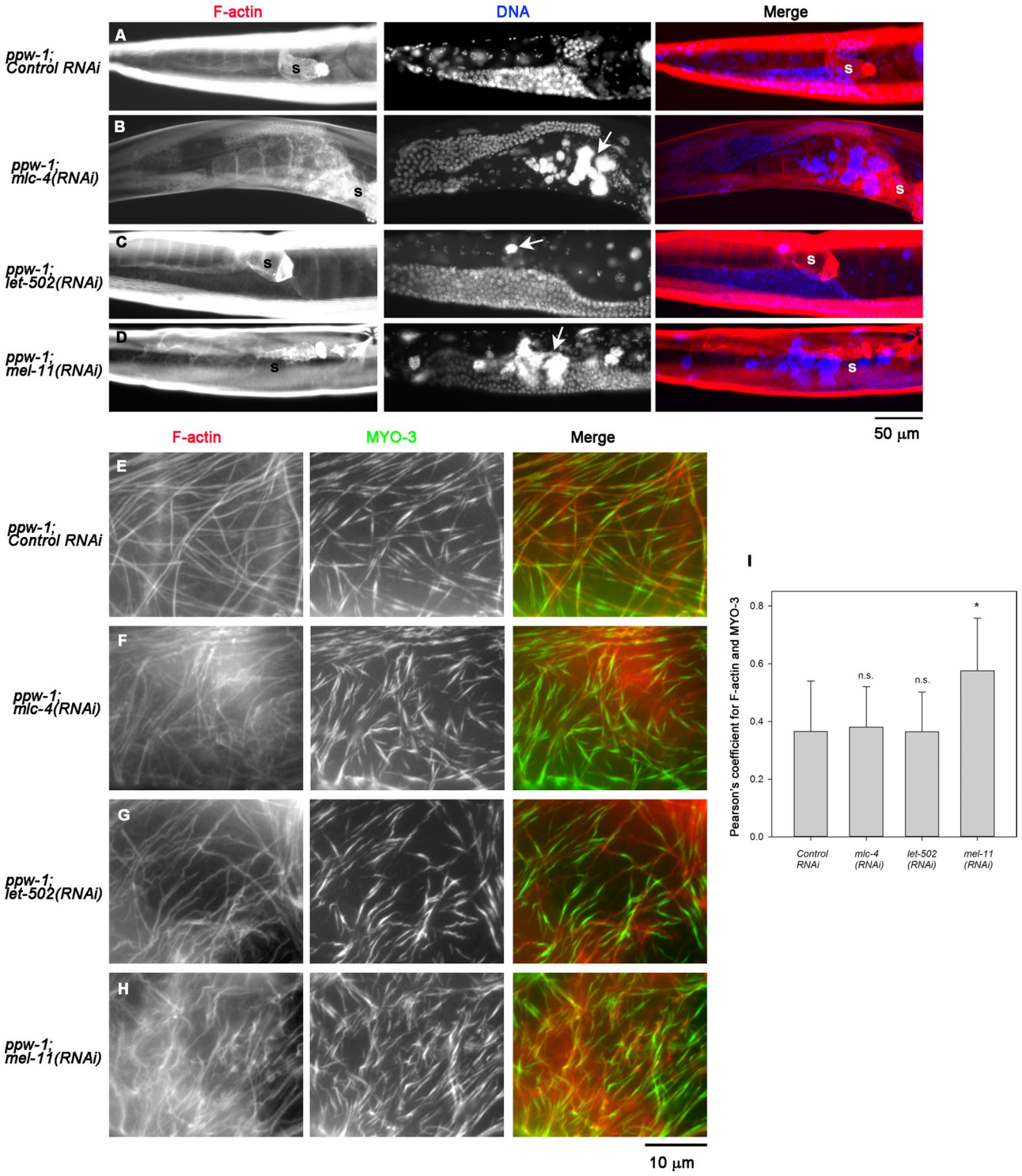

FIGURE 2: MLC-4, LET-502, and MEL-11 are essential for ovulation. *ppw-1* worms were treated with control RNAi (A, E), *mlc-4(RNAi)* (B, F), *let-502(RNAi)* (C, G), or *mel-11(RNAi)* (D, H). (A–D) Whole worms were stained for F-actin (left) and DNA (middle). Right, merged images (F-actin in red and DNA in blue). Ovulation defects were characterized by the presence of endomitotic oocytes (Emo) with large DNA accumulations in the ovary, as indicated by arrows. Positions of the spermatheca are indicated by the letter s. Both *mlc-4(RNAi)* and *mel-11(RNAi)* caused severe Emo phenotypes, whereas *let-502(RNAi)* led to somewhat weaker Emo phenotypes. (E–H) Dissected gonads were stained for F-actin (left) and MYO-3 (middle). Right, merged images (F-actin in red and MYO-3 in green). These RNAi treatments did not cause major disorganization of the actin-MYO-3 network. (I) Pearson's coefficient for F-actin and MYO-3 quantified as a measurement of colocalization and shown as average ± SD ($n = 10$). Results of a statistical test by one-way ANOVA for comparisons with control RNAi; n. s., not significant ($p > 0.05$); *$0.05 > p > 0.01$. Only *mel-11(RNAi)* increased the F-actin-MYO-3 colocalization significantly, suggesting that contraction was induced.

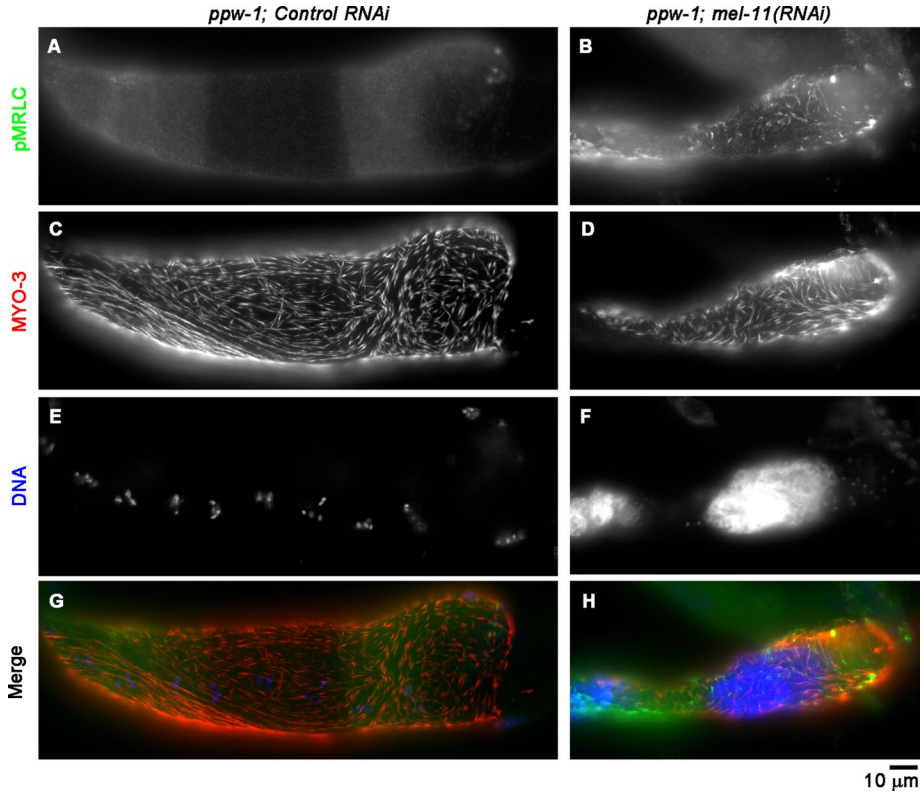

FIGURE 3: Phosphorylation of MRLC is enhanced by RNA interference of MEL-11. *ppw-1* worms were treated with control RNAi (A, C, E, G) or *mel-11(RNAi)* (B, D, F, H), and dissected gonads were stained for p-MRLC (A, B), MYO-3 (C, D), and DNA (E, F). (G, H) Merged images (p-MRLC in green, MYO-3 in red, and DNA in blue). *mel-11(RNAi)* caused shortening of the myoepithelial sheath and enhanced p-MRLC staining.

effect of *let-502(RNAi)* might be weak, because strong loss-of-function alleles of *let-502* are known to cause zygotic elongation defects (Wissmann *et al.*, 1997; Gally *et al.*, 2009). However, high penetrance of the *mel-11(RNAi)* phenotype suggests that inactivation of nonmuscle myosin by dephosphorylation of MLC-4 is critical for successful ovulation. Actin filaments and MYO-3 myosin heavy chain were organized into networks in the myoepithelial sheath of wild type (unpublished data) and *ppw-1* with control RNAi (Figure 2E), and *let-502(RNAi)* did not cause major changes in their organization (Figure 2G). However, *mel-11(RNAi)* caused a denser appearance of MYO-3 filaments (Figure 2H), which is consistent with enhanced actomyosin contractility. MYO-3 is located in the middle of thick filaments, where fewer actin filaments reach (analogous to the M-line regions in sarcomeres; Ono *et al.*, 2007). Therefore actomyosin contraction should increase the overlap between MYO-3 and F-actin. We quantified colocalization of MYO-3 and F-actin in each sample by measuring PC and found that only *mel-11(RNAi)* significantly increased MYO-3/F-actin colocalization (Figure 2I). The data strongly suggest that actomyosin contraction was enhanced by the knockdown of myosin phosphatase containing MEL-11.

To determine whether MLC-4 is regulated by phosphorylation and dephosphorylation, we examined levels of phosphorylated MRLC (p-MRLC) in the myoepithelial sheath, using anti-p-MRLC antibody, which has been used to detect phospho–MLC-4 in *C. elegans* (Lee *et al.*, 2006). In gonads with control RNAi (Figure 3A) or *let-502(RNAi)* (unpublished results), p-MRLC was nearly undetectable, suggesting that basal levels of MLC-4 phosphorylation were very low. However, *mel-11(RNAi)* significantly increased the level of p-MRLC in the myoepithelial sheath (Figure 3B). In addition, the myoepithelial sheath was shrunken and appeared excessively contracted (compare Figure 3, C and D). These results indicate that a myosin phosphatase containing MEL-11 as a myosin-binding subunit is responsible for mediating dephosphorylation of MLC-4 and relaxation of the myoepithelial sheath.

To test directly whether dephosphorylation of MLC-4 is required for ovulation, we examined effects of a phosphomimetic mutant of MLC-4. Phosphorylation of mammalian MRLC at Thr-18 and Ser-19 activates myosin II molecules (Sellers, 1991). These residues are conserved in *C. elegans* MLC-4 as Thr-17 and Ser-18, and a phosphomimetic mutant MLC-4 (T17D, S18D; MLC-4(DD)) has been shown to provide actomyosin-based tissue contractility during embryonic elongation (Gally *et al.*, 2009). Gally *et al.* (2009) reported that GFP–MLC-4(WT) or GFP-MLC-4(DD) rescued embryonic and larval development in an *mlc-4*–null background. However, *mlc-4*–null homozygotes rescued by either transgene became adults with poorly developed gonads (unpublished data). Therefore we examined GFP–MLC-4(WT) or GFP–MLC-4(DD) in *mlc-4/+* heterozygotes, in which a wild-type *mlc-4* is provided by a balancer chromosome. GFP–MLC-4(WT) localized to puncta of relatively uniform size and intensity (Figure 4A). However, GFP–MLC-4(DD) localized to puncta with heterogeneous size and intensity (Figure 4B). Some of the intense puncta of GFP–MLC-4(DD) were correlated with locations where actin filaments accumulated (Figure 4, D and H, arrows), suggesting that contraction of the actin networks was induced by GFP–MLC-4(DD). Of importance, 14.6 ± 8.1% (n = 3) of worms expressing GFP–MLC-4(WT) had endomitotic oocytes, whereas 64.9 ± 1.4% (n = 3) of worms expressing GFP–MLC-4(DD) had endomitotic oocytes (Figure 4F). The relatively high percentage of ovulation defects in worms expressing GFP–MLC-4(WT) could be due to segregation of *mlc-4*–null homozygotes. Although phosphorylation of MLC-4 can induce contraction of actin networks in the myoepithelial sheath, complete or nearly complete dephosphorylation of MLC-4 is important to induce relaxation of the myoepithelial sheath for successful ovulation. Thus these results indicate that cycles of contraction and relaxation of the myoepithelial sheath are regulated by MLC-4 phosphorylation and dephosphorylation by LET-502 and MEL-11 and required for successful ovulation.

Two myosin II populations coordinate actomyosin contractility during ovulation

Previous studies and our present work demonstrate that two distinct myosin II populations are involved in myoepithelial sheath contraction during ovulation: large, needle-like myosin containing UNC-54 and MYO-3 heavy chains (Ardizzi and Epstein, 1987; Rose *et al.*, 1997; Ono *et al.*, 2007) and small, dot-like myosin containing NMY-2 heavy chain and MLC-4 MRLC (this work). To determine whether these two myosin II populations coordinate to generate contractility,

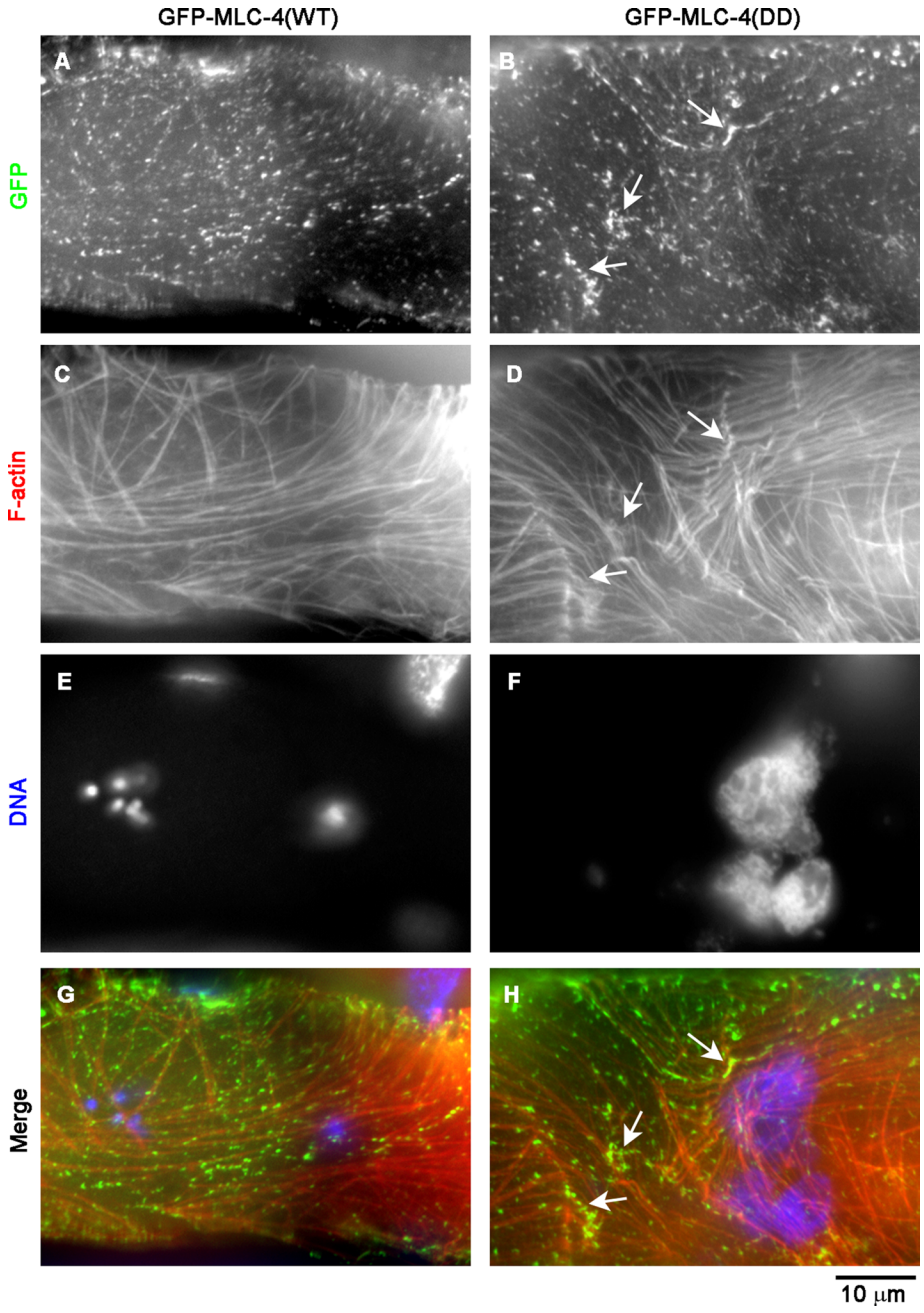

FIGURE 4: Phosphomimetic MLC-4 mutant impairs ovulation. Dissected gonads from *mlc-4/+* worms expressing GFP–MLC-4(WT) (ML1150; A, C, E, G) or GFP–MLC-4(DD) (ML1151; B, D, F, H) were stained for GFP (A, B), F-actin (C, D), and DNA (E, F). Regions of the myoepithelial sheath. Large aggregates of DNA in F indicate the presence of endomitotic oocytes. Arrows indicate locally concentrated GFP–MLC-4(DD) and F-actin, suggesting that the constitutively active MLC-4 mutant induced contraction of the actomyosin networks.

we compared ovulation phenotypes when one or two myosin II populations are disturbed. The MYO-3 heavy chain is essential for organization of contractile apparatuses, and mutation or RNAi of MYO-3 causes embryonic lethality (Waterston, 1989) or severe ovulation defects (Ono *et al.*, 2007). Therefore we used *unc-54(s95)*, a point mutation near the ATP-binding site of the head of the UNC-54 myosin heavy chain, which does not affect organization of contractile apparatuses (Moerman *et al.*, 1982; Dibb *et al.*, 1985). *unc-54(e190)*, a null allele, or *myo-3(RNAi)* causes disorganization of actomyosin networks (Rose *et al.*, 1997; Ono *et al.*, 2007). Although the *unc-54(s95)* mutation by itself does not cause an ovulation defect, it partially suppresses hypercontraction phenotypes in the myoepithelial sheath in troponin I or *unc-87* mutants (Obinata *et al.*, 2010; Ono *et al.*, 2015), indicating that the *unc-54(s95)* mutation weakens contractility produced by the UNC-54 myosin heavy chain.

Control RNAi did not cause ovulation defects in *ppw-1* or *unc-54(s95) ppw-1* (Figure 5, A, B, and J), whereas *mlc-4(RNAi)* caused 100% ovulation defects in either *ppw-1* or *unc-54(s95); ppw-1* (Figure 5, C, D, and I). However, ovulation defects caused by RNAi of *let-502* (ROCK) were greatly enhanced by the *unc-54(s95)* mutation in both appearance of the endomitotic oocytes (compare Figure 5, E and F) and occurrence of ovulation-defective worms (Figure 5I). This result suggests that the low penetrance of the *let-502(RNAi)* phenotype was partly due to an alternative actomyosin contractility produced by UNC-54. In contrast, the rate of ovulation defects caused by RNAi of *mel-11* (myosin-binding subunit of MRLC phosphatase) was slightly reduced by the *unc-54(s95)* mutation (Figure 5I), although the appearance of the endomitotic oocytes was not obviously altered (Figure 5, G and H). Therefore reduced contractility by the *unc-54(s95)* mutation could counterbalance excessive contractility due to lack of MLC-4 dephosphorylation, which partially suppresses the ovulation defects. Together these results suggest that each of the two myosin II populations provides partially compensatory actomyosin contractility of the myoepithelial sheath and that proper regulation of the two myosin systems is essential for successful ovulation in *C. elegans*.

To dissect functions of the two myosin populations during ovulation, we analyzed ovulation processes in live worms by time-lapse Nomarski microscopy (Figure 6). In a normal ovulation process, the myoepithelial sheath initiates intense contraction after oocyte maturation (characterized by nuclear envelope breakdown [NEBD] in an oocyte) and expels the mature oocyte into the spermatheca, where fertilization takes place (McCarter *et al.*, 1997). The *ppw-1* worms with control RNAi showed normal ovulation (seven of seven; Figure 6A). Contraction of the myoepithelial sheath was significantly more frequent at the ovulatory phase (after nuclear NEBD) than at the basal phase (before NEBD; Figure 6I). The *unc-54(s95) ppw-1* worms with control RNAi also completed successful ovulation (11 of 11; Figure 6B). However, enhancement of ovulatory myoepithelial sheath contraction was not statistically significant (Figure 6I). Therefore the UNC-54 myosin is important for increasing ovulatory myoepithelial contraction, but other myosin isoform(s) are sufficient to produce enough forces to complete ovulation. In *ppw*-1, RNAi of *mlc-4* (Figure 6C) or *mel-11* (Figure 6G) caused severe

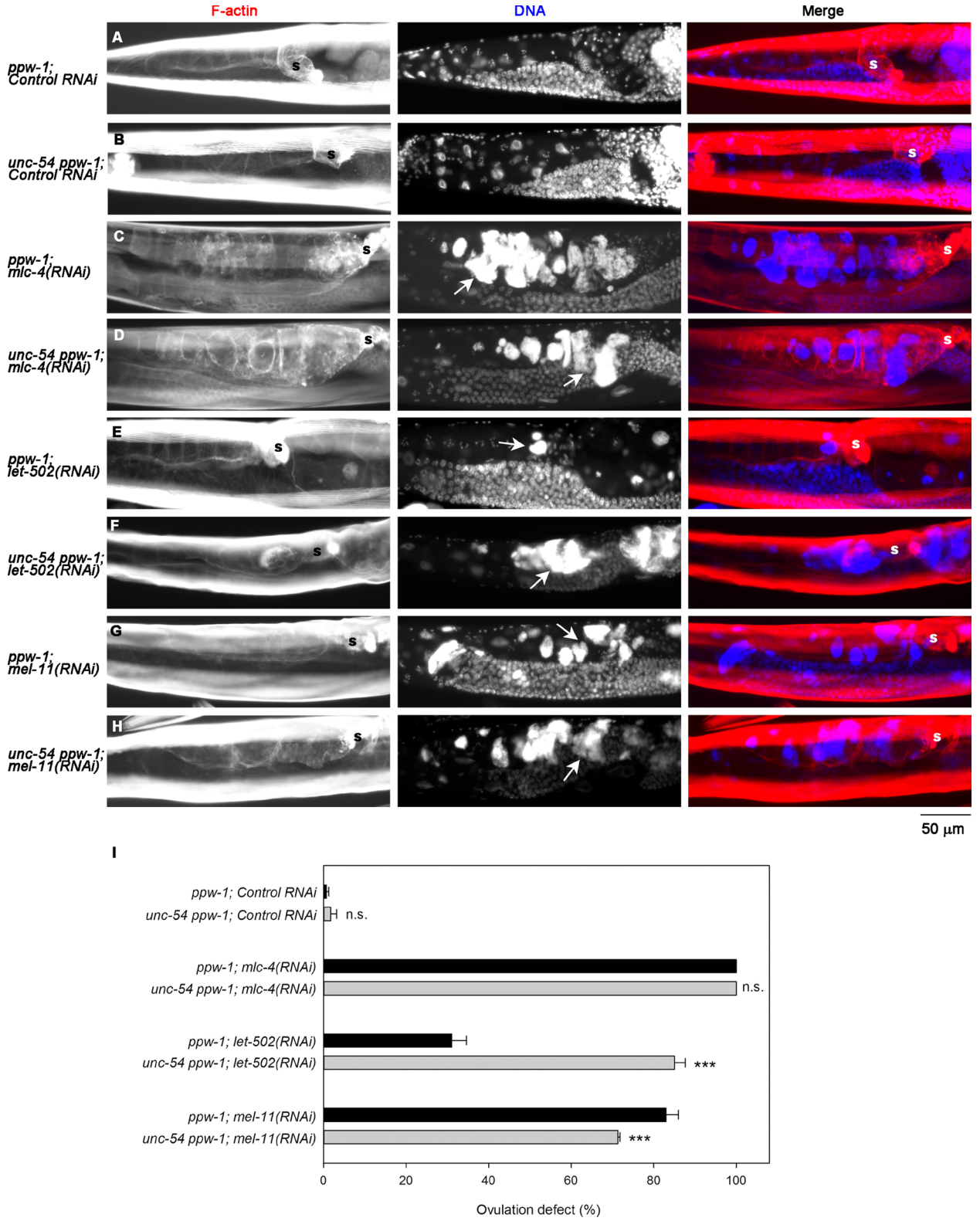

FIGURE 5: The striated muscle myosin isoform (UNC-54) is partially redundant with the nonmuscle myosin isoform. *ppw-1* or *unc-54 ppw-1* worms were treated with control RNAi (A, B), *mlc-4(RNAi)* (C, D), *let-502(RNAi)* (E, F), or *mel-11(RNAi)* (G, H). (A–H) Whole worms were stained for F-actin (left) and DNA (middle). Right, merged images (F-actin in red and DNA in blue). Ovulation defects were characterized by the Emo phenotype as indicated by arrows. Positions of the spermatheca are indicated by the letter s. (I) Percentages of worms with ovulation defects as characterized by the Emo phenotype were scored for 100 worms each after 3 d of RNAi treatment. Data are average ± SD ($n = 3$). Results of a statistical test by one-way ANOVA for comparisons between *ppw-1* and *unc-54 ppw-1*: n. s., not significant ($p > 0.05$); ***$p < 0.001$. The *unc-54* mutation enhanced the ovulation defect of *let-502(RNAi)* but partially suppressed that of *mel-11(RNAi)*.

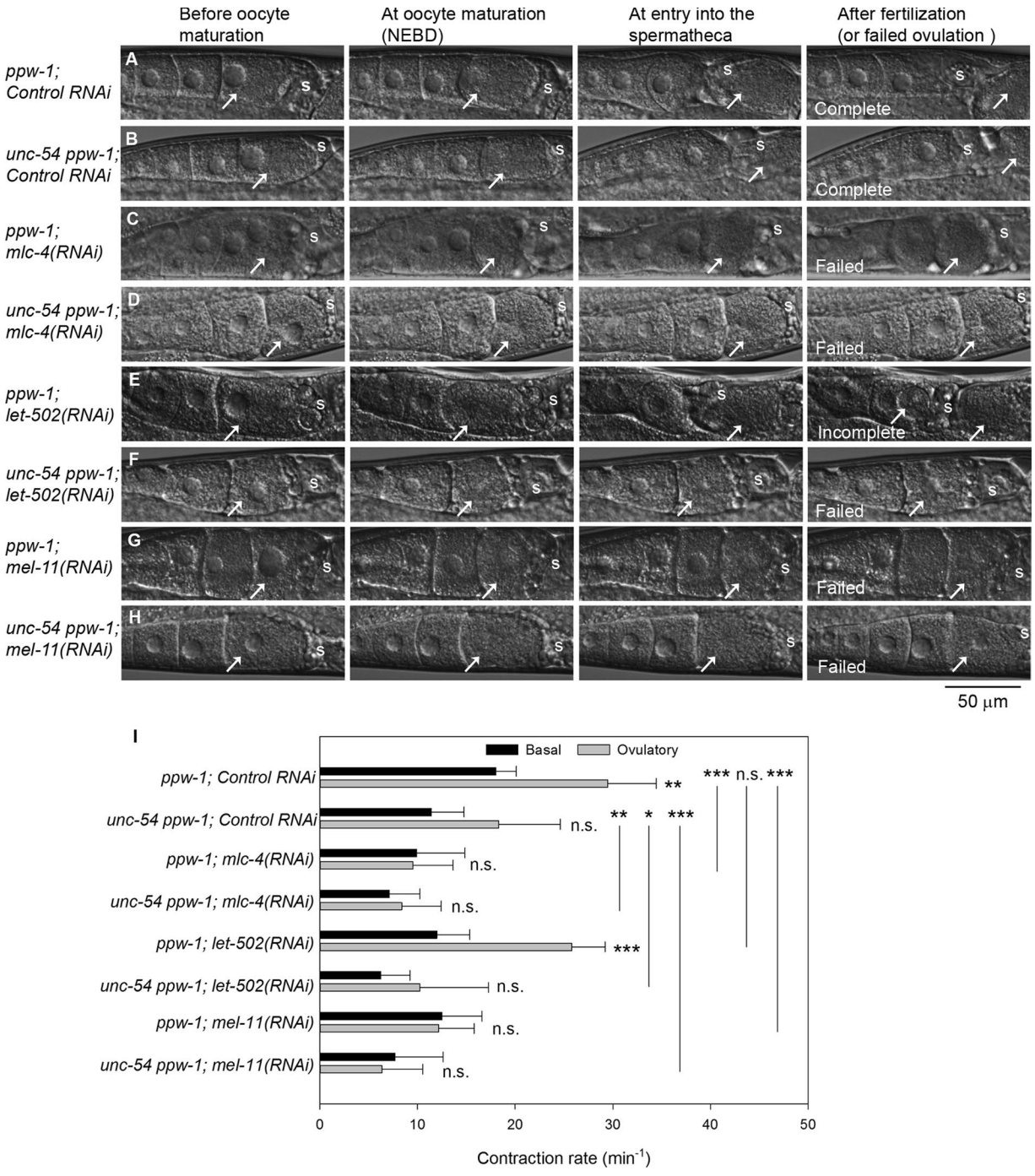

FIGURE 6: Muscle and nonmuscle myosin isoforms regulate enhancement of ovulatory myoepithelial contraction. (A–H) Ovulation processes in live worms were recorded by time-lapse Nomarski microscopy (the most-proximal oocytes are marked by arrows). For each genotype and RNAi treatment (indicated on the left), five to nine animals were examined. Representative snapshots at key steps: before oocyte maturation (nuclei are visible in the most-proximal oocytes), at oocyte maturation (NEBD), at entry into the spermatheca (positions of the spermatheca are indicated by the letter s), and after fertilization (or failed ovulation). Both *ppw-1* and *unc-54 ppw-1* with control RNAi completed ovulation (A, B). However, most of the *ppw-1; let-502(RNAi)* worms showed incomplete ovulation (E), in which the spermatheca prematurely closed and severed the oocyte. All other worms failed ovulation and retained the mature oocytes in the proximal ovaries (C, D, F, G, H). (I) Rates of myoepithelial contraction quantified from the time-lapse images. Basal (black bars) and ovulatory (gray bars) contractions are defined as before and after NEBD, respectively. Results of a statistical test (one-way ANOVA) for comparisons between basal and ovulatory rates (adjacent to the error bars) and between control RNAi and experimental RNAi (ovulatory rates only for pairs indicated by vertical lines): n. s., not significant ($p > 0.05$); *$0.05 > p > 0.01$; **$0.01 > p > 0.001$; ***$0.001 > p$. Enhancement of ovulatory contraction was inhibited by *mlc-4(RNAi)*, *mel-11(RNAi)*, or the *unc-54* mutation. *let-502(RNAi)* inhibited the enhancement in *unc-54 ppw-1* but not in *ppw-1*.

ovulation defects (six of six for *mlc-4(RNAi)* and seven of seven for *mel-11(RNAi)*), in which mature oocytes remained in the ovary in similar ways to previously reported ovulation failures causing the Emo phenotype (Ono and Ono, 2004, 2014). Similar ovulation defects were observed in *unc-54(s95) ppw*-1 (eight of eight for *mlc-4(RNAi)* and seven of seven for *mel-11(RNAi)*). Both *mlc-4(RNAi)* and *mel-11(RNAi)* eliminated the increase in ovulatory myoepithelial contraction and significantly reduced the frequency of contraction in *ppw-1* and *unc-54(s95) ppw-1* (Figure 6I), suggesting that *mlc-4* and *mel-11* are required for increasing ovulatory myoepithelial contraction. The results did not explain why the *unc-54* mutation partially suppressed the Emo phenotype caused by *mel-11(RNAi)* (Figure 5I). This might be because overall contractile forces rather than frequency in the ovulatory phase might be important for successful ovulation. *let-502(RNAi)* in *ppw-1* caused partial ovulation defects. In five of seven examined worms, the spermatheca closed before complete ovulation and severed the oocyte (Figure 6E, right, arrows). In two of seven examined worms, ovulation appeared normal. *let-502(RNAi)* in *ppw-1* neither prevented enhancement of ovulatory myoepithelial contraction nor reduced ovulatory contraction rates significantly (Figure 6I). However, in *unc-54(s95) ppw-1*, *let-502(RNAi)* caused severe ovulation defects (six of seven; Figure 6H) and inhibited the increase in ovulatory myoepithelial contraction (Figure 6I). Basal contraction rates were also affected by disturbance of the two myosin populations in a similar manner but not as drastically as the ovulatory contraction (statistics not shown). These results are consistent with the observation that the *unc-54* mutation enhances the Emo phenotypes caused by *let-502(RNAi)* (Figure 5I), suggesting that the *unc-54* mutant is more sensitive to the activation state of nonmuscle myosin. Overall these live-imaging studies demonstrate that both muscle and nonmuscle myosin isoforms contribute to increasing myoepithelial contraction during the ovulatory phase.

DISCUSSION

Our identification of MLC-4, LET-502, and MEL-11 as important factors for myoepithelial sheath contraction strongly suggests that the small myosin II filaments containing MLC-4 and NMY-2 are under the control of the RHO-1 small GTPase pathway. Previous work showed that *C. elegans* RHO-1 is essential for ovulation and fertility (Norman *et al.*, 2005; McMullan and Nurrish, 2011; Meighan *et al.*, 2015), but its downstream effectors in ovulation have not been identified. A signaling cascade from Rho GTPase to myosin II is conserved in both nonmuscle and smooth-muscle cells in metazoan species (Somlyo and Somlyo, 2003; Piekny *et al.*, 2005). A GTP-bound form of Rho activates ROCK (Ishizaki *et al.*, 1996), which phosphorylates MRLC to activate myosin II (Amano *et al.*, 1996). ROCK also phosphorylates the myosin-binding subunit of MRLC phosphatase and inhibits the phosphatase activity (Kimura *et al.*, 1996). Therefore a likely signaling during ovulatory contractility of the myoepithelial sheath is that LET-502 (ROCK), which is activated by GTP-bound RHO-1, activates myosin II by phosphorylating MLC-4 (MRLC) and inactivates MRLC phosphatase by phosphorylating MEL-11 (myosin- binding subunit of MRLC phosphatase; Figure 7). A previous study concluded that VAV-1, a Rho/Rac guanine nucleotide exchange factor, regulates ovulatory myoepithelial sheath contractility through IP3-mediated Ca^{2+} signals to trigger UNC-54/MYO-3 contraction (Norman *et al.*, 2005; Figure 7). However, our study suggests that phosphoregulation of MLC-4 is another important downstream event of VAV-1, which can be mediated by the RHO-1 small GTPase and NMY-2 contraction. In *Drosophila* striated muscle, a nonmuscle myosin heavy chain *Zipper* localizes to the Z-discs and is required for sarcomeric assembly of muscle myosin and F-actin (Bloor and Kiehart, 2001; Rui *et al.*, 2010), but how these two myosin populations function together to regulate contractility and sarcomere assembly remains unclear. Similar functional coordination of multiple myosin isoforms may be used in other biological processes.

The *let-502(RNAi)* phenotype was relatively weak, with low penetrance of ovulation defects (Figure 2C). This can be partly explained by an alternative actomyosin contractility generated by UNC-54 myosin heavy chain (Figures 5 and 6). In addition, we cannot exclude the possibility that an additional mechanism(s) to activate myosin II containing MLC-4 is important during ovulation or that the RNAi effect was weak. In vertebrates, multiple kinases are known to phosphorylate MRLC to activate or inactivate myosin II (Sellers, 1991; Matsumura *et al.*, 2011). During embryonic elongation in *C. elegans*, three kinases—LET-502, p21-activated kinase (PAK-1), and myotonic dystrophy kinase–related Cdc42-binding kinase (MRCK-1)—act redundantly to regulate MLC-4 in epidermal cells (Gally *et al.*, 2009). Similarly, during ovulation, when *let-502* is depleted, other kinase(s) for MLC-4 might be able to activate myosin II to produce myoepithelial sheath contractility. Because ovulatory contraction of the myoepithelial sheath is a highly coordinated process, multiple mechanisms to control MLC-4 might be important for spatial and temporal regulation of cell contractility.

A myosin II molecule has two heavy chains, two essential light chains, and two MRLCs and forms multimeric bipolar filaments. Spatial segregation of MLC-4 from MYO-3–containing myosin II filaments strongly suggests that each of the two myosin II populations is assembled from specific isoforms of myosin II subunits. Large, needle-like myosin II filaments containing UNC-54 and MYO-3 have paramyosin as a core (Ono *et al.*, 2007). UNC-54 and MYO-3 are the major myosin heavy chains in the body-wall muscle (MacLeod *et al.*, 1981; Miller *et al.*, 1983; Waterston, 1989) and are predicted to coassemble with MLC-1 and MLC-2 as MRLCs (Rushforth *et al.*, 1998) and MLC-3 as an essential light chain (Anderson, 1989). Small, dot-like myosin II filaments containing MLC-4 and NMY-2 probably contain MLC-5 as an essential light chain (Gally *et al.*, 2009). Our preliminary studies indicate that *nmy-2(RNAi)* in *ppw-1* caused only weak ovulation defects (unpublished data), suggesting that NMY-1, another functionally redundant myosin heavy chain (Piekny *et al.*, 2003), might be coassembled with MLC-4 and NMY-2 in the myoepithelial sheath. In the spermatheca, NMY-1 has been shown to be essential for contractility (Kovacevic *et al.*, 2013). Future studies on additional myosin II components and regulatory proteins should help us understand how different myosin II filaments are assembled and regulated in the myoepithelial sheath.

The two distinct myosin II populations appear to generate partially compensatory contractility in the myoepithelial sheath (Figures 5 and 6). However, presumably, they have different biochemical properties and play distinct roles during ovulation. UNC-54 and MYO-3 myosin heavy chains are the major components of the thick filaments in the body-wall muscle, which is obliquely striated muscle (Ono, 2014). In vertebrate striated muscle, such as skeletal and cardiac muscles, myosin in thick filaments is constitutively active, and its association with actin is inhibited at low Ca^{2+} by the actin-bound troponin/tropomyosin complex, which is relieved by high Ca^{2+} (Ebashi, 1984). This allows very rapid on/off switching for muscle contraction by altering the Ca^{2+} levels. Thus the large, needle-like myosin II filaments containing UNC-54 and MYO-3 are probably striated-muscle myosin filaments, which are constitutively active (Figure 7). Indeed, the troponin/tropomyosin complex is essential for ovulatory contraction of the myoepithelial sheath (Myers *et al.*, 1996; Ono and Ono, 2004; Obinata *et al.*, 2010), which can function as a rapid Ca^{2+}-dependent switch for actomyosin contraction

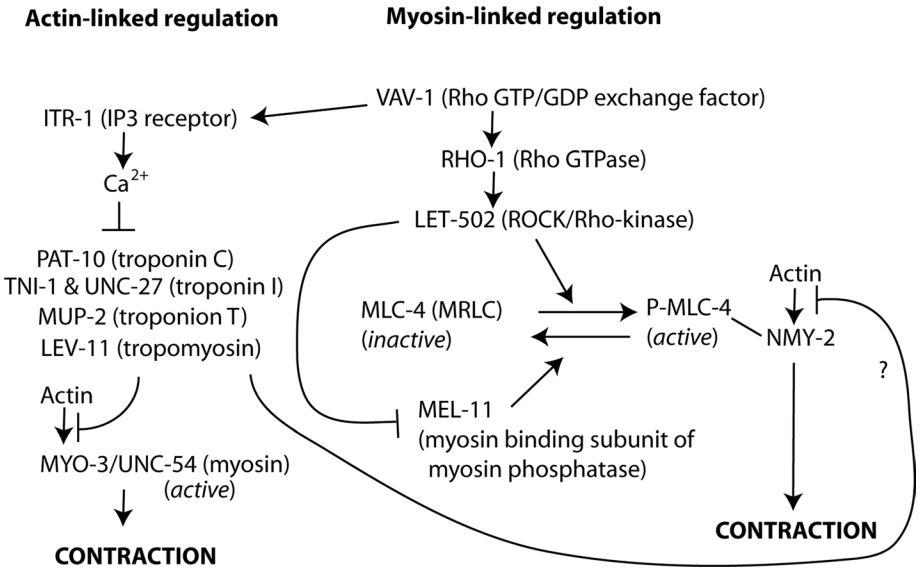

FIGURE 7: Model of regulation of ovulatory contractility in the *C. elegans* myoepithelial sheath. Previous and present studies show that ovulatory contraction is regulated by a hybrid mechanism of classic striated muscle–like actin-linked (left) and nonmuscle/smooth-muscle–like myosin-linked (right) regulations.

(Figure 7). In contrast, regulation of the small myosin II filaments containing MLC-4 depends on phosphorylation and dephosphorylation, which is a relatively slow regulatory mechanism compared with the Ca^{2+} switch. In addition, we recently identified UNC-87B, a calponin-related protein, as a Ca^{2+}-independent, actin-associated inhibitor of myoepithelial sheath contraction with unknown regulatory mechanism (Ono *et al.*, 2015). The myoepithelial sheath exhibits a complex pattern of contraction during ovulation (McCarter *et al.*, 1997), and regulation of actomyosin contractility by multiple mechanisms may allow precise control of tissue contraction and relaxation. In this study, we demonstrated roles of myosins in increasing contraction frequency during the ovulatory phase (Figure 6). In addition, location, timing, and intensity of myoepithelial contraction need to be precisely regulated for successful ovulation. Our analysis did not distinguish different roles of myosin isoforms in ovulation; this will be a subject of future research. In addition, studies to identify additional myosin components and regulatory factors and characterize spatiotemporal regulation of actomyosin contraction will be necessary to understand how cell/tissue contractility is coordinated in the reproductive system.

MATERIALS AND METHODS

Nematode strains

The following *C. elegans* strains were obtained from the *Caenorhabditis* Genetics Center (Minneapolis, MN) and used in this study: N2 wild type, JJ1473 *unc-119(ed3); zuIs45[Pnmy-2::nmy-2::GFP + unc-119(+)]* (Nance *et al.*, 2003), EU573 *orEx2[Pmlc-4::mlc-4::GFP + rol-6(su1006)]* (Shelton *et al.*, 1999), ML1150 *mlc-4(or253)/qC1; mcEx401 [Pmlc-4::GFP::mlc-4(WT) + Ppie-1::GFP::mlc-4(WT) + rol-6(su1006)]* (Gally *et al.*, 2009), ML1151 *mlc-4(or253)/qC1; mcEx402[Pmlc-4::GFP::mlc-4(DD) + Ppie-1::GFP::mlc-4(WT) + rol-6(su1006)]* (Gally *et al.*, 2009), NL2550 *ppw-1(pk2505)* (Tijsterman *et al.*, 2002), and RW5008 *unc-54(s95)*. ON254 *unc-54(s95) ppw-1(pk2505)* was generated by crossing *unc-54(s95)* and *ppw-1(pk2505)* and isolating double homozygotes. Nematodes were grown under standard conditions at 20°C on Nematode Growth Medium agar plates (Stiernagle, 2006).

RNAi experiments

RNAi experiments were performed by feeding with *Escherichia coli* HT115(DE3) expressing double-stranded RNA as described previously (Ono and Ono, 2002). All RNAi experiments except for *mlc-4* were started by treating L4 larvae and observing phenotypes in the next generation. Because *mlc-4(RNAi)* significantly affected larval development and reduced the number of fully developed adult worms, RNAi was started by treating L1 larvae and observing phenotypes when they became adults as described previously (Ono and Ono, 2014). Control RNAi experiments were performed using the unmodified L4440 plasmid vector for feeding RNAi (kindly provided by Andrew Fire, Stanford University, Stanford, CA; Timmons *et al.*, 2001). An RNAi clone for *mlc-4* was kindly provided by Jonathon Howard (Yale University, New Haven, CT; Redemann *et al.*, 2010). RNA clones for *let-502* (I-2I07) and *mel-11* (II-6N17) were obtained from Source BioScience (Nottingham, United Kingdom).

Fluorescence microscopy

Gonads were dissected from adult hermaphrodites on polylysine-coated glass slides as described previously (Ono *et al.*, 2007) and fixed by 4% paraformaldehyde in cytoskeleton buffer (10 mM 2-(*N*-morpholino)ethanesulfonic acid–KOH, pH 6.1, 138 mM KCl, 3 mM $MgCl_2$, 2 mM ethylene glycol tetraacetic acid [EGTA]) containing 0.32 M sucrose and additional 10 mM EGTA (to prevent tissue contraction) for 10 min at room temperature. They were permeabilized with phosphate-buffered saline (PBS) containing 0.5% Triton X-100 and 30 mM glycine for 10 min, reacted with primary antibodies diluted in PBS containing 1% bovine serum albumin and 0.5% Triton X-100 (with or without tetramethylrhodamine-phalloidin), and followed by treatments with secondary antibodies in the same buffer. Primary antibodies used are rabbit anti-GFP polyclonal (600-401-215; Rockland Immunochemicals, Limerick, PA), mouse anti–MYO-3 monoclonal (5-6; Miller *et al.*, 1983), and rabbit anti-p-MRLC (p-Ser-19) polyclonal (3671; Cell Signaling Technology, Danvers, MA). Staining of whole worms with tetramethylrhodamine-phalloidin was performed as described previously (Ono, 2001). 4′,6-Diamidino-2-phenylindole dihydrochloride was included at 0.1 μg/ml in the phalloidin solution to stain DNA. Samples were mounted with ProLong Gold (Life Technologies, Carlsbad, CA) and observed by epifluorescence using a Nikon Eclipse TE2000 inverted microscope (Nikon Instruments, Tokyo, Japan) with a CFI Plan Fluor ELWD 40× (dry; numerical aperture [NA] 0.60) or Plan Apo 60× (oil; NA 1.40) objective. Images were captured by a SPOT RT monochrome charge-coupled device camera (Diagnostic Instruments, Sterling Heights, MI) and processed by IPLab imaging software (BD Biosciences, San Jose, CA) and Photoshop CS3 (Adobe, San Jose, CA). Quantitative image analysis was performed by ImageJ (National Institutes of Health, Bethesda, MD) using the JACoP plug-in (Bolte and Cordelieres, 2006). Pearson's coefficients were analyzed in randomly selected regions of interest (40 × 40 pixels for Figure 1I and 20 × 20 pixels for Figure 2I). Statistical tests (one-way analysis of variance [ANOVA]) were performed using SigmaPlot 13.0 (Systat Software, San Jose, CA).

Time-lapse Nomarski microscopy

Live imaging of the ovulation process was performed essentially as described previously (Ono and Ono, 2014) using a Nikon Eclipse TE2000 inverted microscope with a 40× CFI Plan Fluor objective (NA 1.4, dry). Images were captured at room temperature by a SPOT Idea CMOS camera (Diagnostic Instruments) and recorded at 5 frames/s using the SPOT Imaging Software (Diagnostic Instruments). Movie files were saved in a compressed AVI format at 20 frames/s. Contractions of the proximal ovary were counted at basal (before NEBD) and ovulatory (after NEBD) phases, and contraction rates (per minute) were calculated (n = 5–9). Statistical tests (one-way ANOVA) were performed using SigmaPlot 13.0.

ACKNOWLEDGMENTS

Monoclonal antibody 5-6 (developed by Henry Epstein) was obtained from the Developmental Studies Hybridoma Bank developed under auspices of the National Institute of Child Health and Human Development and maintained by the Department of Biological Sciences, University of Iowa, Iowa City, IA. Some *C. elegans* strains were provided by the *Caenorhabditis* Genetics Center, which is funded by the National Institutes of Health Office of Research Infrastructure Programs (P40 OD010440). This work was supported by a grant from the National Institutes of Health (R01 AR48615) to S.O.

REFERENCES

Amano M, Ito M, Kimura K, Fukata Y, Chihara K, Nakano T, Matsuura Y, Kaibuchi K (1996). Phosphorylation and activation of myosin by Rho-associated kinase (Rho-kinase). J Biol Chem 271, 20246–20249.

Anderson P (1989). Molecular genetics of nematode muscle. Annu Rev Genet 23, 507–525.

Ardizzi JP, Epstein HF (1987). Immunochemical localization of myosin heavy chain isoforms and paramyosin in developmentally and structurally diverse muscle cell types of the nematode *Caenorhabditis elegans*. J Cell Biol 105, 2763–2770.

Beach JR, Hammer JA, 3rd (2015). Myosin II isoform co-assembly and differential regulation in mammalian systems. Exp Cell Res 334, 2–9.

Bloor JW, Kiehart DP (2001). *zipper* nonmuscle myosin-II functions downstream of PS2 integrin in *Drosophila* myogenesis and is necessary for myofibril formation. Dev Biol 239, 215–228.

Bolte S, Cordelieres FP (2006). A guided tour into subcellular colocalization analysis in light microscopy. J Microsc 224, 213–232.

Dibb NJ, Brown DM, Karn J, Moerman DG, Bolten SL, Waterston RH (1985). Sequence analysis of mutations that affect the synthesis, assembly and enzymatic activity of the *unc-54* myosin heavy chain of *Caenorhabditis elegans*. J Mol Biol 183, 543–551.

Ebashi S (1984). Ca^{2+} and the contractile proteins. J Mol Cell Cardiol 16, 129–136.

Gally C, Wissler F, Zahreddine H, Quintin S, Landmann F, Labouesse M (2009). Myosin II regulation during *C. elegans* embryonic elongation: LET-502/ROCK, MRCK-1 and PAK-1, three kinases with different roles. Development 136, 3109–3119.

Hubbard EJ, Greenstein D (2000). The *Caenorhabditis elegans* gonad: a test tube for cell and developmental biology. Dev Dyn 218, 2–22.

Ishizaki T, Maekawa M, Fujisawa K, Okawa K, Iwamatsu A, Fujita A, Watanabe N, Saito Y, Kakizuka A, Morii N, *et al*. (1996). The small GTP-binding protein Rho binds to and activates a 160 kDa Ser/Thr protein kinase homologous to myotonic dystrophy kinase. EMBO J 15, 1885–1893.

Iwasaki K, McCarter J, Francis R, Schedl T (1996). *emo-1*, a *Caenorhabditis elegans* Sec61p gamma homologue, is required for oocyte development and ovulation. J Cell Biol 134, 699–714.

Kachur TM, Audhya A, Pilgrim DB (2008). UNC-45 is required for NMY-2 contractile function in early embryonic polarity establishment and germline cellularization in *C. elegans*. Dev Biol 314, 287–299.

Kimura K, Ito M, Amano M, Chihara K, Fukata Y, Nakafuku M, Yamamori B, Feng J, Nakano T, Okawa K, *et al*. (1996). Regulation of myosin phosphatase by Rho and Rho-associated kinase (Rho-kinase). Science 273, 245–248.

Kovacevic I, Orozco JM, Cram EJ (2013). Filamin and phospholipase C-epsilon are required for calcium signaling in the *Caenorhabditis elegans* spermatheca. PLoS Genet 9, e1003510.

Lee JY, Marston DJ, Walston T, Hardin J, Halberstadt A, Goldstein B (2006). Wnt/Frizzled signaling controls *C. elegans* gastrulation by activating actomyosin contractility. Curr Biol 16, 1986–1997.

MacLeod AR, Karn J, Brenner S (1981). Molecular analysis of the *unc-54* myosin heavy-chain gene of *Caenorhabditis elegans*. Nature 291, 386–390.

Matsumura F, Yamakita Y, Yamashiro S (2011). Myosin light chain kinases and phosphatase in mitosis and cytokinesis. Arch Biochem Biophys 510, 76–82.

McCarter J, Bartlett B, Dang T, Schedl T (1997). Soma-germ cell interactions in *Caenorhabditis elegans*: multiple events of hermaphrodite germline development require the somatic sheath and spermathecal lineages. Dev Biol 181, 121–143.

McMullan R, Nurrish SJ (2011). The RHO-1 RhoGTPase modulates fertility and multiple behaviors in adult *C. elegans*. PLoS One 6, e17265.

Meighan CM, Kelly VE, Krahe EC, Gaeta AJ (2015). alpha integrin cytoplasmic tails can rescue the loss of Rho-family GTPase signaling in the *C. elegans* somatic gonad. Mech Dev 136, 111–122.

Miller DM, Ortiz I, Berliner GC, Epstein HF (1983). Differential localization of two myosins within nematode thick filaments. Cell 34, 477–490.

Miller MA, Nguyen VQ, Lee MH, Kosinski M, Schedl T, Caprioli RM, Greenstein D (2001). A sperm cytoskeletal protein that signals oocyte meiotic maturation and ovulation. Science 291, 2144–2147.

Moerman DG, Plurad S, Waterston RH, Baillie DL (1982). Mutations in the *unc-54* myosin heavy chain gene of *Caenorhabditis elegans* that alter contractility but not muscle structure. Cell 29, 773–781.

Munjal A, Lecuit T (2014). Actomyosin networks and tissue morphogenesis. Development 141, 1789–1793.

Myers CD, Goh PY, Allen TS, Bucher EA, Bogaert T (1996). Developmental genetic analysis of troponin T mutations in striated and nonstriated muscle cells of *Caenorhabditis elegans*. J Cell Biol 132, 1061–1077.

Nance J, Munro EM, Priess JR (2003). *C. elegans* PAR-3 and PAR-6 are required for apicobasal asymmetries associated with cell adhesion and gastrulation. Development 130, 5339–5350.

Norman KR, Fazzio RT, Mellem JE, Espelt MV, Strange K, Beckerle MC, Maricq AV (2005). The Rho/Rac-family guanine nucleotide exchange factor VAV-1 regulates rhythmic behaviors in *C. elegans*. Cell 123, 119–132.

Obinata T, Ono K, Ono S (2010). Troponin I controls ovulatory contraction of non-striated actomyosin networks in the *C. elegans* somatic gonad. J Cell Sci 123, 1557–1566.

Ono S (2001). The *Caenorhabditis elegans unc-78* gene encodes a homologue of actin-interacting protein 1 required for organized assembly of muscle actin filaments. J Cell Biol 152, 1313–1319.

Ono S (2014). Regulation of structure and function of sarcomeric actin filaments in striated muscle of the nematode *Caenorhabditis elegans*. Anat Rec 297, 1548–1559.

Ono K, Obinata T, Yamashiro S, Liu Z, Ono S (2015). UNC-87 isoforms, *Caenorhabditis elegans* calponin-related proteins, interact with both actin and myosin and regulate actomyosin contractility. Mol Biol Cell 26, 1687–1698.

Ono S, Ono K (2002). Tropomyosin inhibits ADF/cofilin-dependent actin filament dynamics. J Cell Biol 156, 1065–1076.

Ono K, Ono S (2004). Tropomyosin and troponin are required for ovarian contraction in the *Caenorhabditis elegans* reproductive system. Mol Biol Cell 15, 2782–2793.

Ono K, Ono S (2014). Two actin-interacting protein 1 isoforms function redundantly in the somatic gonad and are essential for reproduction in *Caenorhabditis elegans*. Cytoskeleton (Hoboken) 71, 36–45.

Ono K, Yu R, Ono S (2007). Structural components of the nonstriated contractile apparatuses in the *Caenorhabditis elegans* gonadal myoepithelial sheath and their essential roles for ovulation. Dev Dyn 236, 1093–1105.

Piekny AJ, Johnson JL, Cham GD, Mains PE (2003). The *Caenorhabditis elegans* nonmuscle myosin genes *nmy-1* and *nmy-2* function as redundant components of the *let-502*/Rho-binding kinase and *mel-11*/myosin phosphatase pathway during embryonic morphogenesis. Development 130, 5695–5704.

Piekny AJ, Mains PE (2002). Rho-binding kinase (LET-502) and myosin phosphatase (MEL-11) regulate cytokinesis in the early *Caenorhabditis elegans* embryo. J Cell Sci 115, 2271–2282.

Piekny A, Werner M, Glotzer M (2005). Cytokinesis: welcome to the Rho zone. Trends Cell Biol 15, 651–658.

Piekny AJ, Wissmann A, Mains PE (2000). Embryonic morphogenesis in *Caenorhabditis elegans* integrates the activity of LET-502 Rho-binding

kinase, MEL-11 myosin phosphatase, DAF-2 insulin receptor and FEM-2 PP2c phosphatase. Genetics 156, 1671–1689.
Redemann S, Pecreaux J, Goehring NW, Khairy K, Stelzer EH, Hyman AA, Howard J (2010). Membrane invaginations reveal cortical sites that pull on mitotic spindles in one-cell *C. elegans* embryos. PLoS One 5, e12301.
Rose KL, Winfrey VP, Hoffman LH, Hall DH, Furuta T, Greenstein D (1997). The POU gene *ceh-18* promotes gonadal sheath cell differentiation and function required for meiotic maturation and ovulation in *Caenorhabditis elegans*. Dev Biol 192, 59–77.
Rui Y, Bai J, Perrimon N (2010). Sarcomere formation occurs by the assembly of multiple latent protein complexes. PLoS Genet 6, e1001208.
Rushforth AM, White CC, Anderson P (1998). Functions of the *Caenorhabditis elegans* regulatory myosin light chain genes *mlc-1* and *mlc-2*. Genetics 150, 1067–1077.
Sellers JR (1991). Regulation of cytoplasmic and smooth muscle myosin. Curr Opin Cell Biol 3, 98–104.
Shelton CA, Carter JC, Ellis GC, Bowerman B (1999). The nonmuscle myosin regulatory light chain gene *mlc-4* is required for cytokinesis, anterior-posterior polarity, and body morphology during *Caenorhabditis elegans* embryogenesis. J Cell Biol 146, 439–451.
Somlyo AP, Somlyo AV (2003). Ca^{2+} sensitivity of smooth muscle and nonmuscle myosin II: modulated by G proteins, kinases, and myosin phosphatase. Physiol Rev 83, 1325–1358.
Stiernagle T (2006). Maintenance of *C. elegans*. WormBook 2006, 1–11.
Strome S (1986). Fluorescence visualization of the distribution of microfilaments in gonads and early embryos of the nematode *Caenorhabditis elegans*. J Cell Biol 103, 2241–2252.
Tijsterman M, Okihara KL, Thijssen K, Plasterk RH (2002). PPW-1, a PAZ/PIWI protein required for efficient germline RNAi, is defective in a natural isolate of *C. elegans*. Curr Biol 12, 1535–1540.
Timmons L, Court DL, Fire A (2001). Ingestion of bacterially expressed dsRNAs can produce specific and potent genetic interference in *Caenorhabditis elegans*. Gene 263, 103–112.
Waterston RH (1989). The minor myosin heavy chain, mhcA, of *Caenorhabditis elegans* is necessary for the initiation of thick filament assembly. EMBO J 8, 3429–3436.
Whitten SJ, Miller MA (2006). The role of gap junctions in *Caenorhabditis elegans* oocyte maturation and fertilization. Dev Biol 301, 432–446.
Wissmann A, Ingles J, Mains PE (1999). The *Caenorhabditis elegans mel-11* myosin phosphatase regulatory subunit affects tissue contraction in the somatic gonad and the embryonic epidermis and genetically interacts with the Rac signaling pathway. Dev Biol 209, 111–127.
Wissmann A, Ingles J, McGhee JD, Mains PE (1997). *Caenorhabditis elegans* LET-502 is related to Rho-binding kinases and human myotonic dystrophy kinase and interacts genetically with a homolog of the regulatory subunit of smooth muscle myosin phosphatase to affect cell shape. Genes Dev 11, 409–422.
Xu X, Guo H, Wycuff DL, Lee M (2007). Role of phosphatidylinositol-4-phosphate 5′ kinase (*ppk-1*) in ovulation of *Caenorhabditis elegans*. Exp Cell Res 313, 2465–2475.
Xu X, Lee D, Shih HY, Seo S, Ahn J, Lee M (2005). Linking integrin to IP_3 signaling is important for ovulation in *Caenorhabditis elegans*. FEBS Lett 579, 549–553.
Yamamoto I, Kosinski ME, Greenstein D (2006). Start me up: cell signaling and the journey from oocyte to embryo in *C. elegans*. Dev Dyn 235, 571–585.
Yin X, Gower NJ, Baylis HA, Strange K (2004). Inositol 1,4,5-trisphosphate signaling regulates rhythmic contractile activity of myoepithelial sheath cells in *Caenorhabditis elegans*. Mol Biol Cell 15, 3938–3949.
Zaidel-Bar R, Zhenhuan G, Luxenburg C (2015). The contractome—a systems view of actomyosin contractility in non-muscle cells. J Cell Sci 128, 2209–2217.